Photoionization spectroscopy of traps in GaN metal-semiconductor field-effect transistors

P. B. Klein,[a] S. C. Binari, J. A. Freitas, Jr., and A. E. Wickenden
Naval Research Laboratory, Washington, DC 20375-5347

(Received 10 March 2000; accepted for publication 20 May 2000)

Measurements of the spectral and intensity dependences of the optically-induced reversal of current collapse in a GaN metal-semiconductor field-effect transistor (MESFET) have been compared to calculated results. The model assumes a net transfer of charge from the conducting channel to trapping states in the high-resistivity region of the device. The reversal, a light-induced increase in the trap-limited drain current, results from the photoionization of trapped carriers and their return to the channel under the influence of the built-in electric field associated with the trapped charge distribution. For a MESFET in which two distinct trapping centers have been spectrally resolved, the experimentally measured dependence upon light intensity was fitted using this model. The two traps were found to have very different photoionization cross-sections but comparable concentrations ($4\times10^{11}\,\mathrm{cm}^{-2}$ and $6\times10^{11}\,\mathrm{cm}^{-2}$), suggesting that both traps contribute comparably to the observed current collapse. [S0021-8979(00)00417-5]

I. INTRODUCTION

Electronic devices based on GaN and AlGaN/GaN heterostructures are of great current interest because of the potential for producing structures that operate at high temperature, high power, high frequency, and in adverse environments. Significant advances have been made in the fabrication of these devices: Nitride-based field-effect transistors (FETs) have been reported to exhibit continuous wave outputs up to 6.9 W/mm[1] and high frequency operation[2] at $f_T=67\,\mathrm{GHz}$ and $f_{\max}=140\,\mathrm{GHz}$. While attainable device characteristics continue to improve, the reproducibility of these characteristics has become problematic,[3] due to device limitations resulting from trapping effects.[3,4] In addition to compensating intentionally doped material, such traps can produce persistent photoconductivity (PPC) effects and current collapse. Current collapse refers to the trapping of charge at defects, after the application of a high drain-source voltage, which results in a significant reduction in the drain current. This effect was recently investigated in a GaN metal-semiconductor field-effect transistor[5] (MESFET), and was observed only after the device had been subjected to a large drain bias. This is consistent with the view that hot carriers were injected into the high-resistivity (HR) GaN layer, where they were trapped by deep centers. Due to the low thermal emission rate from these defects, the trapped carriers remain long after the applied voltage is removed. This transfer of charge produces a depletion region in the channel of the device, which tends to pinch off the device and reduce the drain current. Current collapse has been a significant problem in Si metal-oxide-semiconductor FETs,[6] in AlGaAs/GaAs modulation-doped FETs,[7] and more recently in nitride-based AlGaN/GaN heterostructure FETs[8] (HFETs) and GaN MESFETs.[5,9]

An important characteristic of current collapse is that it is reversible with the application of light: the trapped carriers can be photoionized and are thus released from the traps. Under the influence of the built-in electric field that develops in the space-charge region, the photoionized carriers drift rapidly back to the conducting channel. This reduces the width of the depletion region in the channel and restores the drain current. There have been several investigations of the influence of light on current collapse. Measurement of the spectral dependence of the conductance in AlGaAs/GaAs structures, made before and after the application of a large drain-source voltage, led to the conclusion[10] that the traps responsible for current collapse were localized in the AlGaAs layer. The responsible trap was later identified as the DX center in the AlGaAs.[7] A later probe of AlGaN/GaN devices reported increases in the collapsed drain current due to illumination with near-band gap light and with light near 650 nm,[8] which was associated with an unidentified trap. In studies of current collapse in a GaN MESFET, it was observed[5] that the efficiency of restoring the drain current by light illumination becomes much less effective with increasing wavelength. While current interest is on heterostructure devices because of the high mobility channel formed in these structures, it is also important to understand the nature of the traps in the underlying GaN in order to be able to unravel the contributions to the measured optical response from the various parts of the device structure. Studying current collapse in the simpler GaN MESFET provides a direct way of carrying out this type of study.

In a recent report,[9] we measured the wavelength dependence of the optical restoration of the drain current in a GaN MESFET. Under the initial conditions of full current collapse (i.e., before illumination and with all the traps filled), the fractional increase in the drain current per incident photon was measured as a function of wavelength. This optical response function is related to the photoionization cross section of the trap. The resulting spectrum revealed two distinct

[a]Author to whom correspondence should be addressed; electronic mail: klein@bloch.nrl.navy.mil

Report Documentation Page

Form Approved
OMB No. 0704-0188

Public reporting burden for the collection of information is estimated to average 1 hour per response, including the time for reviewing instructions, searching existing data sources, gathering and maintaining the data needed, and completing and reviewing the collection of information. Send comments regarding this burden estimate or any other aspect of this collection of information, including suggestions for reducing this burden, to Washington Headquarters Services, Directorate for Information Operations and Reports, 1215 Jefferson Davis Highway, Suite 1204, Arlington VA 22202-4302. Respondents should be aware that notwithstanding any other provision of law, no person shall be subject to a penalty for failing to comply with a collection of information if it does not display a currently valid OMB control number.

1. REPORT DATE	2. REPORT TYPE	3. DATES COVERED
MAR 2000		**00-00-2000 to 00-00-2000**

4. TITLE AND SUBTITLE	5a. CONTRACT NUMBER
Photoionization spectroscopy of traps in GaN metal-semiconductor field-effect transistors	5b. GRANT NUMBER
	5c. PROGRAM ELEMENT NUMBER
6. AUTHOR(S)	5d. PROJECT NUMBER
	5e. TASK NUMBER
	5f. WORK UNIT NUMBER
7. PERFORMING ORGANIZATION NAME(S) AND ADDRESS(ES) **Naval Research Laboratory,4555 Overlook Avenue SW,Washington,DC,20375**	8. PERFORMING ORGANIZATION REPORT NUMBER
9. SPONSORING/MONITORING AGENCY NAME(S) AND ADDRESS(ES)	10. SPONSOR/MONITOR'S ACRONYM(S)
	11. SPONSOR/MONITOR'S REPORT NUMBER(S)

12. DISTRIBUTION/AVAILABILITY STATEMENT
Approved for public release; distribution unlimited

13. SUPPLEMENTARY NOTES

14. ABSTRACT

15. SUBJECT TERMS

16. SECURITY CLASSIFICATION OF:			17. LIMITATION OF ABSTRACT	18. NUMBER OF PAGES	19a. NAME OF RESPONSIBLE PERSON
a. REPORT **unclassified**	b. ABSTRACT **unclassified**	c. THIS PAGE **unclassified**	**Same as Report (SAR)**	**10**	

electron traps. Because these spectra were obtained by measuring the optical reversal of current collapse, the two traps observed must be those responsible for this effect. Consequently, this type of spectroscopy can provide signatures for the specific traps that are responsible for current collapse in FET structures.

In this work, we present measurements of the dependence of this effect upon the incident light intensity and develop a detailed model describing the optical restoration of the collapsed drain current. The model establishes a framework for understanding the previously measured spectral dependence and for analyzing the intensity-dependent measurements. This analysis also provides a means of extracting important trap characteristics from the experimental data. In addition, the model determines the relationship between the spectral dependence of the measured response function and that of the trap photoionization cross section.

II. EXPERIMENT

A. Sample and measurement characteristics

Details of the MESFET design and characterization are described in Ref. 5. The FET was fabricated with a drain-source spacing of 5 μm, a gate width of 150 μm and a gate length of 1.5 μm. The 200-nm-thick n-GaN active channel layer was grown on top of a 3-μm-thick, undoped, high-resistivity GaN buffer layer in order to separate the active part of the device from the higher-defect-density material near the sapphire substrate. Hall measurements at 300 K indicated a channel carrier concentration of $2\times10^{17}\,\mathrm{cm}^{-3}$ and a mobility of 410 $\mathrm{cm}^2/\mathrm{V\,s}$. $I-V$ characteristics were determined using a HP4145b semiconductor parameter analyzer, which measures the drain characteristics with a single sweep of the drain-source voltage, V_D, for each gate bias. The current collapse measurements were all carried out at 293 K and at zero gate-source bias. Monochromatic light was provided by a 75 W Xe arc lamp (PTI model A1010) or a tungsten–halogen lamp, and a Spex 1680B 0.22 m double monochromator with a 1200 groove/mm holographic grating. The spectrometer bandpass was set to approximately 3.5 nm. The light was collected with a spherical mirror and focused onto the device. The dependence of the light-induced increase in drain current upon light intensity was determined at a fixed drain voltage, using calibrated neutral density filters to attenuate the incident light.

B. Measurement of drain current restoration

Current collapse occurs after a GaN MESFET is subjected to a high drain-source voltage, and hot carriers are injected into the thick HR GaN layer. The electrons (for an n-channel device) that are trapped in this region by electrically active deep centers produce a charged region in the HR layer, and a corresponding depletion layer extends into the active layer, thus narrowing the channel and causing the $I-V$ characteristic of the device to collapse. In a simplified ''abrupt-junction'' view of this process, the traps, distributed uniformly with concentration N_T, fill to a depth x_T below the n-type/HR interface. This corresponds to the case in which the drain current is fully collapsed, as all of the traps within the charged region are filled. As the device is irradiated with light, trapped carriers are photoionized and drift rapidly back to the channel under the influence of the large built-in electric field ($\approx10^5$ V/cm, see Sec. IV C) that develops across the interface due to the charge transfer. This reduces the amount of trapped charge, shrinks the depletion layer, increases the drain current, and reverses the current collapse.

As the fully collapsed (dark) state corresponds to the traps being completely filled within the charged region of the HR-GaN, a natural measure of the reversal of this phenomenon is the fractional increase in the drain current above the dark level. This is a direct measure of the fraction of trapped carriers that have been released. To be meaningful, this quantity must be normalized by the total number of photons incident on the sample. Consequently, at a fixed value of the drain voltage, we define a response function[9] that is the fractional increase in drain current above the dark level per incident photon of energy $h\upsilon$

$$S(h\upsilon)\equiv\frac{1}{\Phi_{h\upsilon}\cdot t}\cdot\frac{\Delta I(h\upsilon)}{I_{\mathrm{dark}}}. \tag{1}$$

Here $\Phi_{h\upsilon}$ is the incident photon flux, t the illumination time, $\Delta I(h\upsilon)$ the light-induced increase in the drain current above the dark level; $\Delta I(h\upsilon)=[I(h\upsilon)-I_{\mathrm{dark}}]$, where $I(h\upsilon)$ is the drain current after illumination and I_{dark} is the fully collapsed drain current. The product $\Phi_{h\upsilon}\cdot t$ is the total exposure, i.e., the total number of photons per unit area incident on the device after illumination for a time t. In Ref. 9, we noted that under certain circumstances the response function $S(h\upsilon)$ is proportional to the photoionization cross section of the trap, $\sigma(h\upsilon)$. The conditions under which this holds is determined in Sec. IV.

In order to ensure reproducibility, it was important for the measurements to begin with the device in the same state for each measurement. This was accomplished by irradiating the device with a blue GaN light emitting diode (1 mW) before applying the high drain-source bias. This procedure led to very reproducible results, and presumably emptied all of the traps, thus eliminating the channel depletion region and returning the device back to the equilibrium condition.

C. Photoionization spectra

In order to provide a proper context for the intensity-dependent measurements and for the model that will be developed, the previously reported[9] spectral dependence of the optical response function $S(h\upsilon)$ is shown as the open circles in Fig. 1. The same GaN MESFET is used in the present measurements. Two broad absorptions were observed, and labeled Trap 1 and Trap 2. Standard expressions for the spectral dependence of the photoionization cross section of a deep level[11] were unsuccessful in fitting this data. From the apparent large trap depths and the large breadth of these absorptions, it was concluded that the traps were strongly lattice coupled. Consequently, the data were fitted using an expression appropriate for absorption from strongly lattice-coupled defects,[12] shown as the solid line in the figure. Two absorption thresholds were determined, at 1.80 and 2.85 eV below the conduction band, which is suggestive of deep

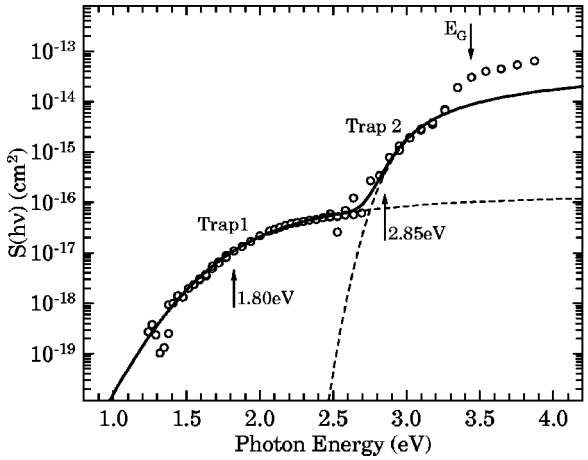

FIG. 1. Spectral dependence of the 293 K response function $S(h\nu)$, which measures the fractional increase in drain current above the dark level per incident photon. Contributions to the absorption are evident from two distinct traps. The solid line is a fit using the spectral dependence of the photoionization cross section appropriate for a defect coupled strongly to the lattice (Ref. 12). The dashed lines indicate the contributions from each of the two traps.

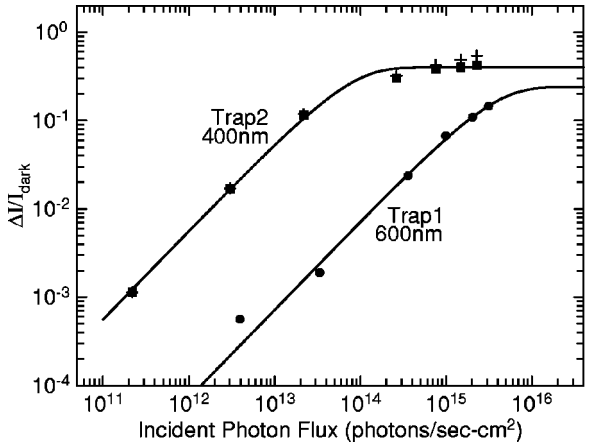

FIG. 2. The fractional increase in the drain current relative to the dark (fully collapsed) level is plotted (data points) against the incident light intensity for 600 nm and 400 nm excitation, which are representative of Trap 1 and Trap 2, respectively. The illumination time was kept constant at 5 s. The solid lines are a fit to the data using Eq. (22). The contribution from Trap 2 is represented by the squares, and was determined by subtracting the relatively small contribution of Trap 1 at 400 nm from the 400 nm Trap 2 data (crosses).

traps. The dashed lines represent the contributions from the individual traps. The additional rise near the band edge was thought to be due to the optical injection of carriers into the channel. Photoionization of charged shallow acceptors is also a possible explanation. Due to the nature of the measurement, it is clear that the two traps evident in Fig. 1 must be those responsible for current collapse in the device. It was also noted[9] that these same traps are most probably associated with PPC effects as well, as each of the two spectra was found to reproduce the photoconductivity spectrum of a trap associated with PPC.[13,14]

In order to study each trap individually through the dependence upon light intensity, a fixed wavelength was chosen for each trap. A wavelength of 600 nm (2.07 eV) was chosen for Trap 1 (see Fig. 1). At this wavelength, the photoinduced increase in the drain current is still reasonably large, but there is no contribution from Trap 2. The spectrum of Trap 2 overlaps completely with contributions from Trap 1. However, the contribution from Trap 2 is dominant at 400 nm (3.10 eV). Consequently, this wavelength was chosen to characterize Trap 2.

III. RESULTS

Available light intensities were limited to $\leqslant 100\ \mu$W spread out over approximately 20 mm^2. The illumination time for all measurements was fixed at $t=5$ s (as in Ref. 9), so that varying the light intensity is equivalent to varying the total exposure, $(\Phi_{h\nu} t)$. In what follows we will often refer to light intensity, the independent variable in the experiment. It should be kept in mind, however, that the change in the charge density due to the optical ejection of carriers from the traps is an *exposure* effect, depending on both the light intensity and the illumination time.

As the dependence of $\Delta I(h\nu)$ upon light intensity was observed at a fixed wavelength, it was equivalent to analyze either $\Delta I(h\nu)/I_{\text{dark}}$ or $S(h\nu)$ [see Eq. (1)], as long as the duration of the illumination remained fixed. The former was chosen as a more intuitive measure, as a saturation of $\Delta I/I_{\text{dark}}$ is expected at high light intensity (exposure), when almost all of the trapped carriers have become liberated. In this same range of light intensities, $S(h\nu)$ decreases as Φ^{-1} due to the intensity normalization built into Eq. (1). The experimentally measured dependence of $\Delta I/I_{\text{dark}}$ on the incident intensity is shown as the data points in Fig. 2. The 400 nm data for Trap 2 (crosses) are corrected (squares) by subtraction of the small contribution from Trap 1 at 400 nm, as discussed in Sec. IV. A linear dependence is observed at low excitation for both traps. At the highest excitations, Trap 2 appears to be well into saturation, while the response of Trap 1 is only beginning to saturate. This is consistent with the much weaker response (by a factor of $\approx 10^2$) of Trap 1 compared to Trap 2 observed in the spectral study shown in Fig. 1. As we will see in Sec. IV, this behavior can be the result of either a smaller photoionization cross section or a lower trap concentration for Trap 1.

IV. MODELING OF CURRENT COLLAPSE

A. Single trapping species

In this section, we will model current collapse in the MESFET in order to develop a framework for understanding this phenomenon in better detail and to enable the extraction of physically significant parameters from the experimental data. We reemphasize that, because the carriers are localized on deep traps, the spatial distribution of charge in the HR layer is effectively ''frozen in''. In what follows, we will emphasize this distinction from the familiar depletion region by using the term ''charged region'' instead. This distinction has clear physical consequences: in a standard p-n junction, as the amount of charge in the depletion layer is reduced (for example, by applying a forward bias), the width of the depletion layer decreases while the volume charge density remains

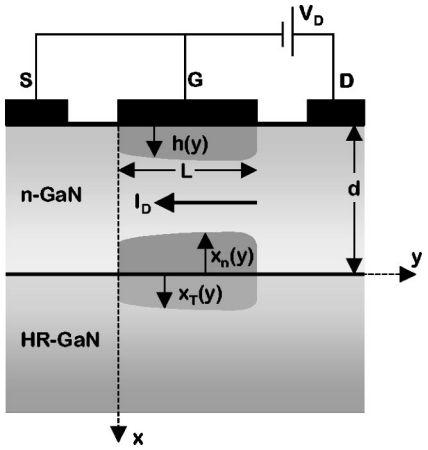

FIG. 3. A sketch of the GaN MESFET is shown with the parameters relevant to the model calculation in Sec. IV. The terms $h(y)$, $x_n(y)$ and $x_T(y)$ represent the variations along the channel of the depths of the gate depletion width, the depletion width at the bottom of the channel, and the width of the charged region, respectively. The depth of the active region is d and the gate length is L.

the same. For the MESFET considered here, this remains the case only for the positively charged depletion layer in the active region. The situation for the charged region is just reversed: the charge within the region is trapped at deep defects. If some of these trapped carriers are liberated, either optically or thermally, and return to the channel, the remaining charges are not free to redistribute. Consequently, the layer width remains the same, and the concentration of trapped charge decreases.

The MESFET will be modeled in a manner similar to typical textbook treatments,[15,16] except that these assume symmetric depletion regions associated with gate contacts at the top and bottom of the device. We will assume the abrupt junction approximation, with uniform densities of dopants in the active region and traps in the HR GaN. The latter are assumed to be neutral when empty and negatively charged when filled. We also assume the gradual channel approximation, appropriate for a 1.5 μm gate length, and with the charge distributed uniformly under the gate.

The device geometry is depicted in Fig. 3. Three charged regions exist: There are depletion regions directly under the gate and at the bottom of the channel (due to the trapped charge), and there is the charged region in the HR GaN layer. After the application of a large drain-source voltage, the *magnitude* of the initial areal charge density on each side of the *n*-type/HR interface, before any light illumination, is given by charge conservation

$$Q_T = eN_d x_n = eN_T x_T, \tag{2}$$

where e is the magnitude of the electronic charge, N_d and N_T are the (uniform) volume concentrations of donors in the channel and traps in the HR region, respectively, and x_n and x_T are the initial widths of the depletion and charged region layers, respectively. Q_T represents the total charge transferred due to the application of the high drain-source voltage. It is assumed that all of the traps in the charged region are initially filled. After illumination with light for a time t, some of the trapped charge is released and returns to the channel, thus decreasing the trapped charge density and the width of the depletion region. The dependence of the areal density of trapped charge on illumination time is given, following Eq. 2, as

$$Q(t) = eN_d x_n(t) = eN^-(t) x_T. \tag{3}$$

The depletion layer width $x_n(t)$ decreases from its initial value x_n as the total amount of trapped charge is reduced by the light illumination. The width of the charged region remains fixed, while the concentration of negatively charged traps, $N^-(t)$, decreases from its initial value N_T as the light releases charge from some of the traps. The concentration of uncharged traps is denoted by $N^0(t)$, so that

$$N^-(t) + N^0(t) = N_T. \tag{4}$$

With this notation, we consider the modeling of current collapse in the MESFET.

With a drain voltage applied, the voltage drop across an incremental section of the channel of length dy and resistance dR is

$$dV = I_D dR = I_D \cdot \frac{dy}{N_d e \mu_n W \cdot [d - x_n(y) - h(y)]}, \tag{5}$$

where μ_n is the mobility of the channel, $V(y)$ is the variation of the applied potential along the length of the device, W the gate width, d the total thickness of the active layer, and h the width of the depletion region under the gate. The expression in square brackets is just the width of the conducting region of the channel, and $N_d e \mu_n$ is the channel conductivity.

Solving Poisson's equation in one dimension and with zero gate voltage (the experimental condition) leads to an expression for the backside depletion width in the channel[15,16]

$$x_n(y) = \sqrt{\frac{2\epsilon}{eN_d}\left(\frac{1}{1 + N_d/N_T}\right) \cdot [U_{\rm bi} + V(y)]}, \tag{6}$$

where $U_{\rm bi}$ is the built-in potential across the *n*-type/HR interface and ϵ is the static dielectric constant of the material. The width of the depletion layer under the gate is given by[15,16]

$$h(y) = \sqrt{\frac{2\epsilon}{eN_d} \cdot [V_{\rm bi} + V(y)]}, \tag{7}$$

with $V_{\rm bi}$ the built-in potential associated with the gate contact. Integrating Eq. (5) over the length of the gate, L, with $V(0) = 0$ and $V(L) = V_D$, the $I-V$ relationship becomes

$$I_D(V_D) = G_0 \cdot \left\{ V_D - \frac{2}{3}\sqrt{\frac{2\epsilon}{eN_d d^2}} \cdot \left[(V_{\rm bi} + V_D)^{3/2} - V_{\rm bi}^{3/2} + \frac{1}{\sqrt{1 + N_d/N_T}} ((U_{\rm bi} + V_D)^{3/2} - U_{\rm bi}^{3/2}) \right] \right\}, \tag{8}$$

where $G_0 = N_d e \mu_n W d/L$ is the conductance of the channel. At low drain voltages, $V_D \ll V_{\rm bi}$, $U_{\rm bi}$, and Eq. (8) becomes linear

$$I_D \cong G_0 V_D \left[1 - \sqrt{\frac{2\epsilon}{eN_d d^2}} \left(\sqrt{V_{\rm bi}} + \frac{1}{\sqrt{1+N_d/N_T}} \sqrt{U_{\rm bi}} \right) \right]. \tag{9}$$

In the linear regime, the depletion widths [Eqs. (6) and (7)] become independent of the applied drain voltage, and depend only on the built-in potential. The measurements described in the previous section were carried out in or near the linear region. Equation 9 expresses the $I-V$ relationship in the linear regime and with no light irradiation: This corresponds to the drain current in the fully collapsed (dark) state, $I_{\rm dark}$. The current collapse is embodied in the built-in potential $U_{\rm bi}$, which is a function of the total areal charge density Q_T [Eq. (2)] injected into the HR region. When the device is illuminated, some of the charge is released from the traps and returns to the channel. With a reduced amount of trapped charge in the HR layer, $U_{\rm bi}$ also decreases. Thus, the built-in potential at the interface, and therefore the drain current, depends upon the amount of light incident upon the device: $U_{\rm bi}=U_{\rm bi}(\Phi,t)$, where Φ and t are the photon flux density (photons/cm^2/s) and duration of the incident light illumination, respectively. The increase in the drain current (at fixed V_D) due to the light is obtained from Eq. (9)

$$\begin{aligned} \Delta I(\Phi,t) &= I_D(\Phi,t) - I_{\rm dark} \\ &= G_0 V_D \sqrt{\frac{2\epsilon}{eN_d d^2}\left(\frac{1}{1+N_d/N_T}\right)} \\ &\quad \cdot [\sqrt{U_{\rm bi}(0,0)} - \sqrt{U_{\rm bi}(\Phi,t)}]. \end{aligned} \tag{10}$$

Before constructing $S(h\nu)$ from Eqs. (1) and (10), it will be convenient to express the built-in potential $U_{\rm bi}$ in terms of the areal density of trapped charge, $Q(t)=eN_d x_n(t)$ [Eq. (3)], where the depletion width in the channel varies with illumination time in response to the decreasing trapped charge density. Combining Eq. (3) with Eq. (6) for the depletion layer width, and noting that in the linear regime x_n is independent of the applied voltage, the built-in potential with light illumination becomes

$$U_{\rm bi}(\Phi,t) = \frac{1+N_d/N_T}{2e\epsilon N_d}[Q(\Phi,t)]^2, \tag{11}$$

while in the dark we have

$$U_{\rm bi}(0,0) = \frac{1+N_d/N_T}{2e\epsilon N_d}[Q(0,0)]^2, \tag{12}$$

where $Q_T \equiv Q(0,0)$ corresponds to the total areal charge density initially transferred into the HR region. Using Eqs. (1) and (9)–(12), the response function for photon flux density $\Phi_{h\nu}$ at photon energy $h\nu$ for illumination time t then becomes

$$S(h\nu,t) = \frac{1}{\Phi_{h\nu}\cdot t} \cdot \left[\frac{Q_T - Q(\Phi_{h\nu},t)}{eN_d d - \sqrt{2e\epsilon N_d V_{\rm bi}} - Q_T} \right]. \tag{13}$$

The denominator of the expression in brackets reflects the areal density of channel carriers, after the depletion regions under the gate and at the HR interface are taken into account.

A determination of the response function $S(h\nu)$ requires evaluating the dependence of the trapped charge density upon the illumination time and intensity. At $t=0$, just before illumination begins, the traps are filled within the charged region, $N^-(0)=N_T$. The areal density of trapped negative charge after light illumination for duration t is [Eq. (3)] $Q(t)=eN^-(t)x_T$, where, as we noted earlier, x_T remains fixed because the remaining trapped charge cannot redistribute. The total charge in the HR layer should also include contributions from the photoexcited carriers in the HR region that have not yet crossed back into the channel. This contribution will be neglected because, as we will show in Sec. V, this concentration is extremely low, as the large built-in field drives the photoexcited carriers rapidly back into the channel layer.

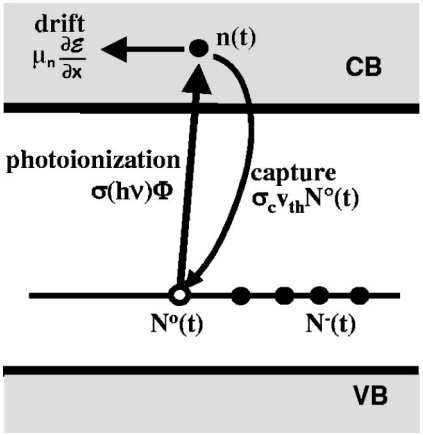

FIG. 4. Schematic level diagram indicating the dominant processes that determine the dynamics of the photoexcited carrier population in the HR GaN region: photoionization, carrier capture, and carrier drift out of the charged region. The illumination-time dependent carrier concentration, neutral trap and charged trap concentrations are given by $n(t)$, $N^0(t)$, and $N^-(t)$, respectively. Terms describing the transition rates for each process are also shown.

In equilibrium, (no trapped charge) the traps can be either empty or partially compensated, depending upon the position of the Fermi level in the HR material. If the traps are partially compensated, the total trap concentration N_T in Eq. (2) must correspond only to the concentration of *uncompensated* traps in equilibrium. The remaining traps that were already filled in equilibrium will not contribute to the current collapse process or to the optical reversal of current collapse, since these processes only depend upon the amount of charge that has been *transferred* from the channel to the HR layer. For example, if all N_T trapped carriers have been photoionized and removed from the charged region, any remaining filled traps, corresponding to those that were already filled in equilibrium, can still be photoionized. However, these photoexcited carriers experience no built-in field, as the region is no longer charged. Consequently, they remain in the HR region and are eventually re-trapped. With these considerations, $N^-(t)$ must correspond only to the traps that were filled as a consequence of the initial application of a high drain-source voltage.

The carrier dynamics associated with the photoionization of traps in the charged region is represented in Fig. 4. Three processes dominate the time dependence of the trapped charge density: photoionization, carrier capture, and carrier

drift back to the conducting channel. The former process generates photoexcited carriers into the conduction band of the HR material, while the latter two processes compete for those carriers. In Sec. V, we will show that for the conditions under which the experiments were carried out, the carrier capture rate is negligible in comparison to the rate of carrier drift. Neglecting carrier capture, $N^-(t)$ takes a particularly simple form

$$N^-(t)=N_T e^{-\sigma(h\nu)\cdot\Phi\cdot t}, \tag{14}$$

where $\sigma(h\nu)$ is the photoionization cross section of the trap. Consequently, we can rewrite Eq. (3) as

$$Q(\Phi,t)=eN_T x_T e^{-\sigma(h\nu)\cdot\Phi\cdot t}=Q_T e^{-\sigma(h\nu)\cdot\Phi\cdot t}. \tag{15}$$

Combining Eqs. (13) and (15), the dependence of the response function on illumination time and intensity becomes

$$S(h\nu,t)=\frac{1}{\Phi_{h\nu}\cdot t}\cdot K\cdot[1-e^{-\sigma(h\nu)\cdot\Phi\cdot t}] \tag{16}$$

with

$$K=\frac{Q_T}{eN_d d-\sqrt{2e\epsilon N_d V_{\rm bi}}-Q_T}, \tag{17}$$

where the parameter K is dependent only upon the initial trapped charge density and the characteristics of the channel. Under conditions of weak carrier excitation (small photoionization cross section or low light exposure), such that $\sigma(h\nu)\cdot\Phi\cdot t\ll 1$, Eq. 16 becomes

$$S(h\nu)\cong K\cdot\sigma(h\nu). \tag{18}$$

Thus, the conditions under which the response function $S(h\nu)$ is proportional to the photoionization cross section of the trap are; (1) that the measurement is made in or near the linear regime, $V_D<V_{\rm bi}$, $U_{\rm bi}$, and (2) that the measurement is made under weak excitation, $\sigma(h\nu)\cdot\Phi\cdot t\ll 1$. The photoionization spectra shown in Fig. 1 were obtained under these conditions.

It is now evident that the response function $S(h\nu)$ is not sufficient to determine whether one of the two traps in Fig. 1 is dominant in causing the observed current collapse. While the spectra in Fig. 1 clearly resolve the responsible traps, the response function only measures how effectively light can *reverse* this effect. The parameter that determines the contribution of a particular trap toward producing current collapse is the concentration of carriers that can be trapped on that defect due to the application of the high drain-source voltage. Equations (2), (17) and (18) indicate that $S(h\nu)$ depends on both the trap concentration and on the photoionization cross section. These parameters are deduced in Sec. IV C by fitting the experimental data to the model developed here.

B. Multiple trap species

For wavelengths longer than about 480 nm ($h\nu<2.6$ eV), the contribution of Trap 1 to $S(h\nu)$ in Fig. 1 is independent of that from Trap 2. For shorter wavelengths, both traps contribute. The model described above can be extended rather simply to the case of overlapping contributions, such as that for $h\nu>2.6$ eV in Fig. 1. Assuming that the charge is distributed over two distinct traps, it is straightforward to show that the response function becomes

$$S(h\nu,t)=\frac{1}{\Phi_{h\nu}\cdot t}\cdot\{K_1\cdot[1-e^{-\sigma_1(h\nu)\cdot\Phi\cdot t}]+K_2\cdot[1-e^{-\sigma_2(h\nu)\cdot\Phi\cdot t}]\}, \tag{19}$$

where

$$K_j=\frac{Q_{jT}}{eN_d d-\sqrt{2e\epsilon N_d V_{\rm bi}}-Q_T}. \tag{20}$$

Here, the $\sigma_j(h\nu)$ and the Q_{jT} are the photoionization cross section and the areal charge density associated with each trap, $j=1,2$, and $Q_T=Q_{1T}+Q_{2T}$ is the total areal charge density [Eq. (2)]. Extension to more than two traps is obvious. For the case of low excitation, $\sigma_j(h\nu)\cdot\Phi\cdot t\ll 1$, and the response function reduces to

$$S(h\nu)\cong K_1\cdot\sigma_1(h\nu)+K_2\cdot\sigma_2(h\nu). \tag{21}$$

Thus, the individual contributions in Fig. 1 are additive under low excitation conditions.

C. Fitting of the intensity dependence

The dependence of the optical reversal of current collapse on the intensity of the incident light for fixed illumination time (Fig. 2), was studied by monitoring $\Delta I(h\nu)/I_{\rm dark}$ rather than $S(h\nu)$, as noted in Sec. III. From Eqs. (1) and (16), this can be written

$$\frac{\Delta I(h\nu)}{I_{\rm dark}}=K\cdot[1-e^{-\sigma(h\nu)\cdot\Phi\cdot t}], \tag{22}$$

where K is a function of the concentration of trapped charge and known channel characteristics [Eq. (17)]. At 400 nm, the response seen in Fig. 2 for Trap 2 (crosses) contains a small contribution from Trap 1 (see Fig. 1) that becomes nonnegligible in the saturation regime. Subtracting this contribution, the squares in Fig. 2 indicate the response associated with Trap 2 alone. For each trap, two parameters are required to fit the data; K and $\sigma(h\nu_{\rm exp})$, where $h\nu_{\rm exp}$ is the photon energy used in the measurement. Equation (22) is plotted as the solid lines in Fig. 2, using the results of this fitting procedure for each of the two traps. The parameter K determines the saturation level, corresponding to having emptied all of the traps, while the magnitude of the data in the linear region is most sensitive to the photoionization cross section. The resulting parameters were found to be: $\sigma_2(400\ {\rm nm})\cong 2.8\times10^{-15}\ {\rm cm}^2$, $K_2\cong 0.40$; $\sigma_1(600\ {\rm nm})\cong 6\times10^{-17}\ {\rm cm}^2$, $K_1\cong 0.24$. Note that the relative photoionization cross sections for the two traps as determined from this procedure are consistent with the spectral measurements of Fig. 1.

From the experimentally determined values of K for each trap, the *areal* trap concentrations $\mathcal{N}_{1T}$ and $\mathcal{N}_{2T}$ ($\mathcal{N}_{jT}\equiv Q_{jT}/e=N_{jT}\cdot x_T$) can be determined using Eq. 20. With $N_d=2\times10^{17}\ {\rm cm}^{-3}$, $d=200$ nm, $V_{\rm bi}=1$ V for the Pt gate contact, and taking $\epsilon\cong 9.5$ for GaN,[17–19] we find that $\mathcal{N}_{1T}$ and $\mathcal{N}_{2T}$ are comparable: $\mathcal{N}_{1T}\cong 4\times10^{11}\ {\rm cm}^{-2}$, $\mathcal{N}_{2T}\cong 6\times10^{11}\ {\rm cm}^{-2}$, and consequently the total areal trap density is $\mathcal{N}_T\cong 1\times10^{12}\,{\rm cm}^{-2}$. It is now clear that the large difference in

the observed magnitudes of $S(h\upsilon)$ for the two traps (Fig. 1) results primarily from the difference in their photoionization cross sections. In contrast, the concentrations of the two traps are comparable. Consequently, both traps contribute comparably to the current collapse in this device.

The maximum field across the *n*-type/HR interface can now be estimated: for the simple abrupt junction described earlier, $\mathcal{E}_{\max}=Q_T/\epsilon=e\cdot\mathcal{N}_T/\epsilon$. We find the field at the interface, $\mathcal{E}_{\max}\cong 2\times 10^5$ V/cm for this device in the fully collapsed state. Thus, the transfer of charge into the HR region produces a rather large initial electric field that drives the carriers rapidly back into the channel when they are released from the traps.

V. CARRIER DYNAMICS

Two simplifying assumptions were made in connection with Eqs. (3) and (14) in determining the dependence upon illumination time of the concentration of filled traps, $N^-(t)$, and of the total areal charge density, $Q(t)$. These assumptions were: (1) that the rate of recapture of photoexcited carriers in the HR region was negligible in comparison to the rate of drift of carriers out of the region, and (2) that the charge density due to photoexcited free carriers in the HR region was negligible compared with the charge density due to trapped carriers. It will be shown that these assumptions are valid except in the limit of very long illumination times, when almost all of the traps have been emptied, and the built-in field has become weak. If the carrier generation rate, $\sigma(h\upsilon)\Phi$, becomes small enough (low optical fluence or small photoionization cross section), thermal emission would also have to be taken into account.

To examine this situation more closely, the dynamics of carrier generation and recombination must be considered. The photoexcited carrier dynamics in the HR GaN was summarized in Fig. 4. Trapped carriers, with concentration $N^-(t)$, are photoionized by the incident light, and may be re-trapped at neutral (uncompensated) centers, with concentration $N^0(t)=N_T-N^-(t)$, or they may be swept out of the charged region by the built-in field before they can be trapped. The current density $\mathbf{J}_n$ associated with the photoexcited carriers can be related to the carrier concentration $n(t)$ in the HR region through the continuity equation

$$\frac{\partial n}{\partial t}=G_n-R_n+\frac{1}{e}\nabla\cdot\mathbf{J}_n, \tag{23}$$

where G_n is the carrier generation rate due to photoionization and R_n is the recombination rate due to re-trapping. As indicated in Fig. 4, we may write

$$G_n=\sigma(h\upsilon)\Phi N^-(t), \tag{24}$$

$$R_n=\sigma_c v_{\text{th}} N^0(t)n(t), \tag{25}$$

where σ_c is the *room temperature* electron capture cross section of the trap, v_{th} is the average electron thermal velocity, $v_{\text{th}}=(3k_BT/m_e^*)^{1/2}$, k_B is Boltzmann's constant, and m_e^* is the electron effective mass of GaN,[20] $m_e^*\cong 0.2m_0$. Because of the high electric field in the charged region, carrier drift effects will dominate carrier diffusion. Under these conditions, Eq. (23) simplifies to

$$\frac{\partial n}{\partial t}=G_n-R_n+n\mu_e\frac{\partial\mathcal{E}}{\partial x}, \tag{26}$$

where $\mathcal{E}$ is the built-in electric field and μ_e the electron mobility in the HR GaN. Note that the very low mobility observed in HR GaN, generally associated with a deep-defect hopping conductivity mechanism,[21] is appropriate only for *thermally* generated carriers. The mobility of *photoexcited* carriers would be expected to be closer to that measured in the *n*-type layer.

Under the abrupt junction approximation with uniform charge densities, $\mathcal{E}(x)$ is linear in x. Taking the total volume charge density in the HR region as $-e[N^-(t)+n(t)]$, which allows contributions from both charged traps and photoexcited carriers, we find that $\partial\mathcal{E}/\partial x=-e[N^-(t)+n(t)]/\epsilon$. Combining this with Eqs. (24)–(26), the time-dependent carrier concentration is determined by

$$\frac{dn}{dt}=\sigma(h\upsilon)\Phi N^-(t)-\{aN^0(t)+b[N^-(t)+n(t)]\}n(t), \tag{27}$$

where $a\equiv\sigma_c v_{\text{th}}$ and $b\equiv(\mu_e e/\epsilon)$ are representative of the capture and drift processes, respectively. The competition between capture and drift is evident in the term enclosed in curly brackets. The corresponding concentration of negatively charged traps is determined by

$$\frac{dN^-}{dt}=-\sigma(h\upsilon)\Phi N^-(t)+aN^0(t)n(t). \tag{28}$$

If we first consider the case where recapture of the photoexcited carriers is neglected ($a=0$), Eq. (28) leads directly to the exponential decay of the trapped carrier concentration indicated in Eq. (14). The solution of Eq. (27) for $n(t)$ in this situation results in a carrier concentration that rises rapidly with a time constant $(bN_T)^{-1}$ to a constant level, $n_{\text{ss}}=[\sigma(h\upsilon)\Phi/b]$, determined by a quasisteady-state balance between carrier generation and carrier drift.[22] Assuming a typical trap concentration of $10^{16}\,\text{cm}^{-3}$ for Trap 2 [$\sigma_2(400\,\text{nm})\approx 2.8\times 10^{-15}\,\text{cm}^2$], the carrier concentration is found to rise with a characteristic time of about 1 psec to a maximum quasisteady-state value (for the highest optical fluence employed in this work) of approximately $n_{\text{ss}}\approx 6\times 10^4\,\text{cm}^{-3}$. This is shown as the inset in Fig. 5 for an incident photon flux of $\Phi=5\times 10^{13}\,\text{cm}^{-2}\,\text{s}^{-1}$ (see, e.g., Fig. 2). It thus becomes clear from the magnitude of n_{ss} that the charge density associated with the free carrier concentration remains much smaller than that associated with the filled traps, until the latter are almost all empty. Consequently, the neglect of the free carriers in determining the charge density of the HR region is seen to be a very reasonable approximation.

For carrier capture to be negligible, the capture term in Eq. (27) must be much smaller than the drift term. Taking into account that $n(t)\ll N_T$, this condition becomes

$$\left(\frac{a}{b}\right)\cdot\left[\frac{N^0(t)}{N^-(t)}\right]\ll 1. \tag{29}$$

The condition under which this inequality remains valid is determined by the magnitude of (a/b). Evaluating this ex-

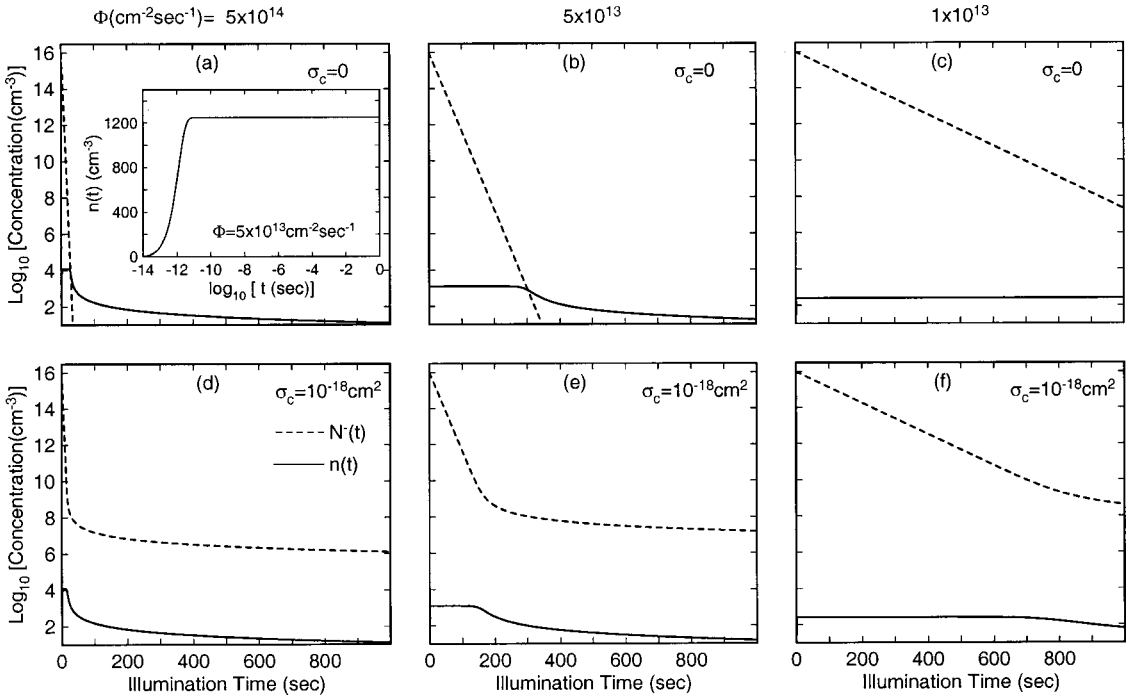

FIG. 5. The dependence upon illumination time of the photoexcited carrier concentration, $n(t)$, and the charged trap concentration, $N^-(t)$, calculated by solving Eqs. (27) and (28) simultaneously by numerical methods. The top row (a,b,c) corresponds to a trap with a negligible capture cross section, while the bottom row (d,e,f) corresponds to a room temperature capture cross section $\sigma_c = 1\times10^{-18}\,\mathrm{cm}^2$. Three values of the incident photon flux Φ are indicated, corresponding with increasing excitation to linear, intermediate, and saturation regimes, as observed for Trap 2 in Fig. 2. The optical exposure in these calculations is varied at fixed light intensity by varying the illumination time. The inset shows the development of the quasisteady-state carrier concentration on the picosecond time scale, calculated for intermediate excitation conditions, $\Phi = 5\times10^{13}\,\mathrm{cm}^{-2}\,\mathrm{s}^{-1}$.

pression requires knowledge of the room temperature capture cross section of the traps being investigated in this work.

While such data are not available for the traps considered here, capture cross sections in HR and *n*-type GaN have been reported[23–25] in a broad range from roughly 10^{-23} cm^2 to 10^{-15} cm^2. Polyakov *et al.*[25] have reported capture cross sections for GaN near room temperature for the E2 center $[\sigma_c(278\,\mathrm{K}) = 4\times10^{-20}\ \mathrm{cm}^2]$ and the E4 center $[\sigma_c(385\,\mathrm{K}) = 3.3\times10^{-23}\ \mathrm{cm}^2]$. In Ref. 9 we presented evidence to suggest that the two traps observed in this work also participate in PPC. As PPC due to traps generally involves centers with small capture cross sections, it follows that the traps in Fig. 1 would also be expected to have small capture cross sections. Hirsch *et al.*[13] confirm this, concluding from their PPC measurements that the trap corresponding to Trap 2 in the current work would need to have a very small capture cross section. With these considerations in mind, we choose a capture cross section of $1\times10^{-18}\,\mathrm{cm}^2$ as an appropriate compromise to estimate (a/b) for Trap 2. This value is small compared to the largest capture cross sections, yet not so small as to preclude any significant re-trapping.

Using this value for σ_c, a mobility comparable to that in the *n*-GaN channel, and with the 300 °K thermal velocity for GaN, $v_{\mathrm{th}} \cong 9\times10^6\,\mathrm{cm/s}$, we find $(a/b) \approx 1\times10^{-7}$. This suggests that, even with uncertainty in some of the parameters, the inequality given by Eq. (29) remains valid until virtually all of the charged traps have been neutralized. Consequently, the neglect of carrier trapping is of concern only at very long illumination times and does not have a significant effect on the analysis of the data in Fig. 2.

These considerations may be investigated in more detail by solving the coupled equations (26) and (27) simultaneously, and without further approximations, using numerical methods. The result of this computation is shown in Fig. 5. The concentrations of $N^-(t)$ (dashed line) and $n(t)$ (solid line) are plotted versus illumination time for three values of the incident light flux; 5×10^{14}, 5×10^{13}, and 1×10^{13} $\mathrm{cm}^{-2}\,\mathrm{s}^{-1}$, which correspond to saturation, intermediate and linear regimes, respectively, for Trap 2 in the intensity dependent measurements shown in Fig. 2. The top row of panels corresponds to the case with negligible re-trapping, while the bottom row corresponds to a room temperature capture cross section of $1\times10^{-18}\,\mathrm{cm}^2$. For the time scale in this figure, the carrier concentration is initially constant at its quasisteady-state value, $[\sigma(h\nu)\Phi/b]$, as shown in the inset. Without carrier capture, the trapped carrier concentration decays exponentially with irradiation time, while the carrier concentration remains constant until the filled trap concentration has decayed to the point where $N^-(t) \approx n(t)$. At this stage, $N^-(t)$ no longer dominates the contribution to the charge density that determines the built-in electric field. Beyond this point the quasisteady-state carrier concentration can no longer be supported, and $n(t)$ begins to decay. As expected, more intense light leads to a faster decay of the filled trap concentration, and thus to an earlier decay of the carrier concentration.

The bottom row of panels in Fig. 5 corresponds to a nonzero capture cross section. There is little effect of capture on the carrier and filled trap concentrations at short illumination times. Capture effects become significant at later

times, when the inequality in Eq. (29) is no longer satisfied. It can be shown that this same condition also corresponds to $N^-(t)$ becoming nonexponential, as the recapture of photoionized carriers slows the decay of the trapped carrier concentration. With stronger excitation, capture becomes significant at earlier illumination times. At later times, when there is significant re-trapping of the photoionized carriers, the quasisteady-state balance of photoionization and drift is disrupted, and the carrier concentration begins to decay. This occurs when the fraction of filled traps, $N^-(t)/N_T$, has decreased sufficiently so as to be comparable with the fraction (a/b), and almost all of the traps have been emptied. At even later times, when capture dominates over drift, $n(t)$ follows a t^{-1} behavior. It should be noted that these considerations apply to time scales that are substantially longer than the 5 s illumination time employed in the measurements of Figs. 1 and 2. The experimental conditions correspond to a quasisteady-state carrier concentration and an exponentially decaying filled trap concentration.

VI. DISCUSSION

The experimental technique discussed in this work has been shown to provide spectroscopic signatures of traps that degrade FET output characteristics by limiting the drain current. By modeling the current collapse process, important trap characteristics such as the areal trap density and the photoionization cross section can be obtained. Of greater significance, the model provides a framework for understanding the process and for applying the technique. The main limitation of the measurement, of course, is that it is sensitive only to current collapse and to traps that participate in that process. In some sense, this is also an attribute, as it is clear that any traps observed in this way can be unambiguously identified as contributors to this effect. This limitation should not be considered absolute, in the sense that the general approach may be extended to any trap-related phenomenon that responds to light illumination. Photocapacitance spectroscopy is an obvious example.

When extracting physical parameters using the model developed in Sec. IV, it is most suitable to use a gateless structure, as the gate tends to block some of the light, thus leading to an overestimate of the incident light intensity. When such structures are not available, as in the present case, it can be shown that this effect will lead to an underestimate of the extracted photoionization cross sections by the same factor, but will have no significant effect on the extracted areal trap concentrations or on the spectral dependence of the photoionization cross section (Fig. 1).

While the use of a gateless structure would be ideal, there are several approaches that could be employed with gated structures. One solution is to use a semitransparent gate. While FETs are not generally fabricated in this way, it would be possible to produce test structures in this manner. As the substrates are transparent to light, another alternative would be to allow the light to enter from the bottom of the device. However, this limits the available wavelengths to those below the band gap of GaN, which could become problematic in studies of AlGaN/GaN structures. Bottom-access measurements have been used to probe the actual location of traps in a device structure: Dang *et al.*[26] measured the spectral dependence of photoconductivity in a PPC study of an AlGaN/GaN structure, comparing results from top and bottom access in an effort to determine the location (AlGaN or GaN) of traps associated with features in the photoconductivity spectrum. It was concluded that defects giving rise to PPC were present in both the AlGaN and the GaN layer. While some features could be associated with a particular layer, the location of other spectral features that were below the gap of both materials could not be distinguished. The broad absorption observed at longer wavelengths was interpreted in terms of a broad distribution of defect states within the band gap. Such a broad distribution is not required, however, in order to account for this kind of absorption spectrum. As we have noted[9] in reference to the two broad absorptions in Fig. 1, such broad bands can result quite naturally from a single deep defect that is strongly coupled to the lattice.

Using a very different approach, Nguyen, Nguyen, and Grider[3] investigated the location of traps in an AlGaN/GaN heterostructure FET by observing a reduction in current compression with increasing negative gate bias. They concluded from this that the traps resided either in the AlGaN layer or at the interface. A similar conclusion was determined for AlGaAs/GaAs modulation-doped FETs[10] over a decade ago. Recently, Trassaert *et al.*[4] have observed the effects of surface states in their GaN MESFETs. This conclusion was based on the lack of any difference in threshold voltage between static and pulsed measurement conditions.

Because of the simplicity of the MESFET structure, the traps in the current investigation can reside only in the HR GaN layer, at the channel/HR-GaN interface, or as surface states. We do not believe that surface states or surface charges can account for the observed current collapse. First, the gate lag response, which is generally associated with surfaces,[27] shows little dependence on the magnitude of the applied drain-source voltage in GaN high electron mobility transistors (HEMTs).[28] This is unlike the current collapse mechanism reported here, that requires a high drain-source voltage. Furthermore, silicon nitride passivation of GaN HEMTs has resulted in a change of the gate lag response,[29] with no effect on the observed current collapse behavior. In addition, devices fabricated on conductive buffer layers do not exhibit current collapse.[29] This is a further indication that this phenomenon is due to charge trapping in the buffer layer.

The responsible traps cannot reside in the active region, as empty electron traps would simply be compensated by the channel carriers, with or without the high drain-source voltage. Their effect would be only to diminish the carrier concentration in the channel. In this work, we have assumed that the traps are in the bulk of the HR GaN. Such traps can result from point defects within single GaN grains, or they can be associated with extended defects, such as deep centers localized within the core of a threading edge dislocation.[30] As we noted earlier, both of the traps that were observed through photoionization spectroscopy exhibit the same optical absorption signatures as those of defects observed to be respon-

sible for PPC, and it is very likely that they are the same defects. In both cases the PPC studies were carried out on thick GaN layers grown on sapphire.[13,14] No conducting channel/HR GaN interface was present. It is therefore unlikely that the traps studied in this work, which we believe to be the same PPC centers, are located at the interface. If it were assumed, however, that the traps reside only at the interface, it is straightforward to show that the analysis described in Secs. IV and V remains essentially unchanged: The areal charge density $eN^-(t)x_T$ in the charged region of the HR GaN is replaced by $e\mathcal{N}(t)$, where $\mathcal{N}(t)$ is the areal density of filled traps at the interface.

VII. SUMMARY

The dependence upon light intensity (exposure) of the reversal of current collapse was measured in a GaN MESFET for two distinct trapping centers. In order to extract meaningful parameters from the data, the process was modeled as resulting from the photoionization of trapped carriers in the HR GaN layer and the subsequent return of these carriers to the channel under the influence of the built-in electric field at the HR/channel interface. The modeling procedure also determined the conditions under which the optical response function $S(h\nu)$, that measures the reversal of current collapse, is proportional to the photoionization cross section of the trap: These conditions are: (1) that the device is operated in the linear regime, and (2) that the measurements are carried out at low optical excitation. The effect of the recapture of the photoionized carriers on the validity of the proposed model was also considered. It was found that for the traps considered here, which are expected to have a relatively small capture cross section, carrier capture becomes important only at long illumination times, when virtually all of the trapped carriers have been returned to the channel. Using the model developed here, the experimental data were fitted, yielding a capture cross section and an areal trap concentration for each of the traps: $\sigma_1 \cong 6\times10^{-17}$ cm^2, $\mathcal{N}_1 \cong 4\times10^{11}$ cm^{-2}; $\sigma_2 \cong 2.8\times10^{-15}$ cm^2, $\mathcal{N}_2 \cong 6\times10^{11}$ cm^{-2}. Thus, the two traps occur with comparable concentrations, and contribute comparably to the current collapse. The large difference in their measured optical response, $S(h\nu)$, was found to be due to the large difference in their photoionization cross sections.

ACKNOWLEDGMENTS

The authors wish to thank J. Albrecht for helpful comments and for a critical reading of the manuscript, and P. Ruden and W. Kruppa for several helpful conversations. This work was sponsored in part by the Office of Naval Research.

[1] S. T. Sheppard, K. Doverspike, W. L. Pribble, S. T. Allen, J. W. Palmour, L. T. Kehias, and T. J. Jenkins, IEEE Electron Device Lett. **20**, 161 (1999).
[2] L. F. Eastman, K. Chu, J. Smart, and J. R. Shealy, Mater. Res. Soc. Symp. Proc. **512**, 3 (1998).
[3] C. Nguyen, N. X. Nguyen, and D. E. Grider, Electron. Lett. **35**, 1380 (1999).
[4] S. Trassaert, B. Boudart, C. Gaquière, D. Théron, Y. Crosnier, F. Huet, and M. A. Poisson, Electron. Lett. **35**, 1356 (1999).
[5] S. C. Binari, W. Kruppa, H. B. Dietrich, G. Kelner A. E. Wickenden, and J. A. Freitas, Jr., Solid-State Electron. **41**, 1549 (1997).
[6] T. H. Ning, C. M. Osburn, and N. H. Yu, J. Electron. Mater. **6**, 65 (1977); L. Forbes, E. Sun, R. Alders, and J. Moll, IEEE Trans. Electron Devices **ED-26**, 1816 (1979).
[7] A. Kastalsky and R. A. Kiehl, IEEE Trans. Electron Devices **ED-33**, 414 (1986); R. Fisher, T. J. Drummond, J. Klem, W. Kopp, T. S. Henderson, D. Perrachione, and J. Morkoç, *ibid.* **ED-31**, 1028 (1984).
[8] M. A. Khan, M. S. Shur, Q. C. Chen, and J. N. Kuznia, Electron. Lett. **30**, 2175 (1994).
[9] P. B. Klein, J. A. Freitas, Jr., S. C. Binari, and A. E. Wickenden, Appl. Phys. Lett. **75**, 4016 (1999).
[10] R. Fisher, T. J. Drummond, W. Kopp, H. Morkoç, K. Lee, and M. Shur, Electron. Lett. **19**, 789 (1983).
[11] J. C. Inkson, J. Phys. C **14**, 1093 (1981).
[12] D. V. Lang, R. A. Logan, and M. Jaros, Phys. Rev. B **19**, 1015 (1979); P. M. Mooney, G. A. Northrup, T. N. Morgan, and H. G. Grimmeiss, *ibid.* **37**, 8298 (1988).
[13] M. T. Hirsch, J. A. Wolk, W. Walukiewicz, and E. E. Haller, Appl. Phys. Lett. **71**, 1098 (1997).
[14] C. V. Reddy, K. Balakrishnan, H. Okumura, and S. Yoshida, Appl. Phys. Lett. **73**, 244 (1998).
[15] S. M. Sze, *Physics of Semiconductor Devices* (Wiley, New York, 1981), p. 77.
[16] A. S. Grove, *Physics and Technology of Semiconductor Devices* (Wiley, New York, 1967), p. 159.
[17] K. Matsubara and T. Takagi, Jpn. J. Appl. Phys., Part 1 **22**, 511 (1982).
[18] A. S. Barker and M. Ilegems, Phys. Rev. B **7**, 743 (1973).
[19] H. Morkoç, S. Strite, G. B. Gao, M. E. Lin, B. Sverdlob, and M. Burns, J. Appl. Phys. **76**, 1363 (1994).
[20] G. D. Chen, M. Smith, J. Y. Lin, H. X. Jiang, S.-H. Wei, M. A. Khan, and C. J. Sun, Appl. Phys. Lett. **68**, 2784 (1996).
[21] D. C. Look, D. C. Reynolds, W. Kim, Ö. Aktas, A. Botchkarev, A. Salvador, and H. Morkoç, J. Appl. Phys. **80**, 2960 (1996); D. C. Look, D. C. Reynolds, R. L. Jones, W. Kim, Ö. Aktas, A. Botchkarev, A. Salvador, and H. Morkoç, Mater. Sci. Eng., B **44**, 423 (1997).
[22] For $a=0$ and $t \ll (\sigma\Phi)^{-1}$, $N^-(t) \cong N_T$, and Eq. (27) reduces to $dn/dt = \sigma\Phi N_T - bN_T n - bn^2$. In the limit $(\sigma\Phi/b) \ll N_T$, which is clearly the present case ($\sigma\Phi/b < 10^5$ cm^{-3}), this can be solved to yield $n(t) = (\sigma\Phi/b)[1-\exp(-bN_T t)]$, which describes exponential growth at a rate bN_T and saturation to a level $\sigma\Phi/b$.
[23] D. C. Look, Z.-Q. Fang, W. Kim, Ö. Aktas, A. Botchkarev, A. Salvador, and H. Morkoç, Appl. Phys. Lett. **68**, 3775 (1996).
[24] Z.-Q. Fang, D. C. Look, W. Kim, Z. Fan, A. Botchkarev, A. Salvador, and H. Morkoç, Appl. Phys. Lett. **72**, 2277 (1998); P. Hacke, T. Detchprohm, K. Hiramatsu, N. Sawaki, K. Tadatomo, and K. Miyake, J. Appl. Phys. **76**, 304 (1994).
[25] A. Y. Polyakov, N. B. Smirnov, A. S. Usikov, A. V. Govorkov, and B. V. Pushniy, Solid-State Electron. **42**, 1959 (1998).
[26] X. Z. Dang, C. D. Wajng, E. T. Yu, K. S. Boutros, and J. M. Redwing, Appl. Phys. Lett. **72**, 2745 (1998).
[27] J. C. M. Hwang, Solid-State Electron. **43**, 1325 (1999).
[28] S. C. Binari, K. Ikossi-Anastasiou, W. Kruppa, H. B. Dietrich, G. Kelner, R. L. Henry, D. D. Koleske, and A. E. Wickenden, Mater. Res. Soc. Symp. Proc. **572**, 541 (1999).
[29] S. C. Binari, K. Ikossi-Anastasiou, J. A. Roussos, D. Park, D. D. Koleske, A. E. Wickenden, and R. L. Henry, Proceedings, 2000 International Conference on GaAs Manufacturing Technology (in press).
[30] K. Leung, A. F. Wright, and E. B. Stechel, Appl. Phys. Lett. **74**, 2495 (1999).